J Biomol NMR (2012) 54:307–316
DOI 10.1007/s10858-012-9673-y

ARTICLE

A spectroscopic assignment technique for membrane proteins reconstituted in magnetically aligned bicelles

Wenxing Tang · Robert W. Knox · Alexander A. Nevzorov

Received: 18 May 2012 / Accepted: 6 September 2012 / Published online: 14 September 2012

Abstract Oriented-sample NMR (OS-NMR) has emerged as a powerful tool for the structure determination of membrane proteins in their physiological environments. However, the traditional spectroscopic assignment method in OS NMR that uses the "shotgun" approach, though effective, is quite labor- and time-consuming as it is based on the preparation of multiple selectively labeled samples. Here we demonstrate that, by using a combination of the spin exchange under mismatched Hartmann-Hahn conditions and a recent sensitivity-enhancement REP-CP sequence, spectroscopic assignment of solid-state NMR spectra of Pf1 coat protein reconstituted in magnetically aligned bicelles can be significantly improved. This method yields a two-dimensional spin-exchanged version of the SAMPI4 spectrum correlating the ^{15}N chemical shift and ^{15}N–^{1}H dipolar couplings, as well as spin-correlations between the (i, $i \pm 1$) amide sites. Combining the spin-exchanged SAMPI4 spectrum with the original SAMPI4 experiment makes it possible to establish sequential assignments, and this technique is generally applicable to other uniaxially aligned membrane proteins. Inclusion of an ^{15}N–^{15}N correlation spectrum into the assignment process helps establish correlations between the peaks in crowded or ambiguous spectral regions of the spin-exchanged SAMPI4 experiment. Notably, unlike the traditional method, only a uniformly labeled protein sample is required for spectroscopic assignment with perhaps only a few selectively labeled "seed" spectra. Simulations for the magnetization transfer between the dilute spins under mismatched Hartmann Hahn conditions for various B_1 fields have also been performed. The results adequately describe the optimal conditions for establishing the cross peaks, thus eliminating the need for lengthy experimental optimizations.

Keywords Oriented-sample NMR (OS-NMR) · Cross-polarization · Membrane proteins · Pf1 · Spectroscopic assignment · Magnetically aligned bicelles · Mismatched Hartmann Hahn conditions

Abbreviations

DMPC	1,2-Dimyristoyl-*sn*-glycero-3-phosphocholine
DHPC	1,2-Dihexanoyl-*sn*-glycero-3-phosphocholine
6-*O*-PC	1,2-Di-*O*-hexyl-*sn*-glycero-3-phosphocholine
SAMPI4	SAMMY pulse sequence with $\pi/4$ pulse correction
PISA	Polarity index slant angles
REP-CP	Repetitive cross-polarization
MMHH	Mismatched Hartmann-Hahn
PDSD	Proton-driven spin diffusion

Introduction

Magnetically oriented bicelles (Sanders et al. 1994; Glover et al. 2001; De Angelis and Opella 2007) provide a high degree of macroscopic alignment thus yielding sharp resonance lines that can be used for structure determination of bicelle-reconstituted membrane proteins. Moreover, bicelles provide a native-like environment for the embedded proteins including complete hydration, high lipid-to-protein ratios, and a near-physiological temperature range. In their natural aligned state, the DMPC/DHPC

Electronic supplementary material The online version of this article (doi:10.1007/s10858-012-9673-y) contains supplementary material, which is available to authorized users.

W. Tang · R. W. Knox · A. A. Nevzorov (✉)
Department of Chemistry, North Carolina State University, 2620 Yarbrough Drive, Raleigh, NC 27695-8204, USA
e-mail: alex_nevzorov@ncsu.edu

bicelles orient so that their membrane normals are perpendicular to the aligning magnetic field. Though it is possible to 'flip' the bicelles with the addition of lanthanide ions (Prosser et al. 1996), thus making the bicelle normals parallel to the external magnetic field, unflipped bicelles yields sharper resonance lines. This is due to the fact that the range for the motionally averaged dipolar couplings and proton chemical shift anisotropy is narrower at the perpendicular orientation, thus making proton decoupling more efficient and the effect of the mosaic spread less pronounced. Here the structural information is provided by the uniaxially averaged chemical shift anisotropies and dipolar couplings due to the fast rotational diffusion of membrane proteins about their alignment axis (the bilayer normal) (Park et al. 2006a; Nevzorov 2011). Previous studies (Park et al. 2006a; Cady and Hong 2009) have estimated the correlation time of the uniaxial diffusion to be on the microsecond time scale.

Pf1 coat protein is composed of 46 amino acids (4.6 kDa), and is the major protein of Pf1 bacteriophage. It has a relatively simple structure: two alpha helices connected by a loop with the Q16–A46 region spanning the membrane (Park et al. 2010). In its membrane-bound form, it assists the virus exit from the infected bacterial cells and its assembly by coating the phage virion (Nambudripad et al. 1991). The structure of Pf1 coat protein reconstituted in magnetically aligned bicelles has been recently reported (Park et al. 2010). Two-dimensional solid-state ^{15}N NMR spectra of Pf1 were found to contain resolved resonances for the residues Q16–A46 (Park et al. 2010). Spectroscopic assignment of the ^{15}N NMR spectra has been accomplished by detecting the positions of the resonances for selectively labeled samples followed by the application of the "shotgun" approach (Park et al. 2010). The latter still remains the current principal assignment method in oriented-sample NMR (OS NMR) as it provides nearly absolute assignment. However, it is generally restricted to the main secondary-structure elements such as alpha-helix (Marassi and Opella 2000; Wang et al. 2000) and beta-sheet (Marassi 2001). In addition, this method requires preparation of multiple selectively labeled samples, making it time consuming and expensive. Hence, a purely spectroscopic method of assignment utilizing uniformly labeled samples would greatly increase the value of OS NMR for structure determination of membrane proteins of arbitrary topology. A method involving cross-referencing of the anisotropic chemical shifts at the perpendicular and parallel sample orientations has been proposed (De Angelis et al. 2006; Lu et al. 2011). However, this method requires the knowledge of the corresponding isotropic chemical shifts for each residue, thus necessitating additional solution NMR experiments. Alternatively, proton-driven spin diffusion (PDSD) (Suter and Ernst 1985) can be used to establish cross-correlations between the neighboring spins, thus providing a spectroscopic assignment method similar to those routinely used in solution and MAS NMR. In recent years, various spectroscopic methods based on dilute spin exchange (Marassi et al. 1999; Xu et al. 2011) have been implemented to establish sequence-specific resonance assignments. Very recently, the ^{15}N OS NMR spectrum of sarcolipin has been assigned in "flipped" bicelles (Mote et al. 2011), where the membrane normal is parallel to the external magnetic field. In order to achieve higher spectral resolution, a three-dimensional pulse sequence employing PDSD was utilized. However, the PDSD-based methods suffer from the requirement of long mixing intervals (up to several seconds) in order to establish detectable spin-exchange signals among the weakly coupled dilute ^{15}N nuclei, thus potentially resulting in missing cross peaks. As an alternative to circumvent the above issue, an analog of the proton-assisted recoupling experiment (Lewandowski et al. 2007) has been developed for aligned samples (Nevzorov 2008) with the potential of providing a general spectroscopic assignment method in OS NMR. This method is based on the transfer of the magnetization between the rare spins (^{15}N or ^{13}C) under mismatched Hartmann-Hahn (MMHH) conditions. The magnetization transfer utilizing MMHH conditions is accomplished with the assistance of the proton spin bath, and does not depend on the direct coupling between the low spins (Nevzorov 2008). Under the MMHH conditions, the Zeeman order of energy for an ^{15}N spin is transferred into the dipolar order of the proton bath and then back to the Zeeman order of the neighboring ^{15}N spins (Khitrin et al. 2011), thus establishing cross peaks in a multidimensional NMR spectrum. Based on the results obtained for an *n*-acetyl leucine (NAL) single crystal, this scheme is capable of establishing correlations among the dilute spins (^{15}N) separated by as far as 6.7 Å. Such an ability would be of great value for the spectroscopic assignment of solid-state NMR spectra of oriented membrane proteins. Additionally, the contact time in the MMHH scheme is only several milliseconds, which dramatically shortens the overall experiment time as compared to PDSD-based spin exchange, which require the contact times of several seconds. Furthermore, the MMHH method has been extended to the measurement of heteronuclear dipolar couplings by inclusion of the SAMPI4 pulse sequence (Nevzorov and Opella 2007) in the indirect dimension, thus yielding a spin-exchanged high-resolution separated local-field spectrum (Nevzorov 2009). In a previous study, the MMHH method has demonstrated its applicability for the uniformly labeled Pf1 phage when the axis of the sample alignment is parallel to the magnetic field (Knox et al. 2010). In principle, the method is applicable to any macroscopically aligned dilute-spin system bridged by a strong proton dipolar network, thus providing a general strategy for the sequential assignment of resonances in NMR spectra of oriented membrane proteins.

In the present work, we apply the MMHH technique to establish spin-correlations for membrane proteins at the

perpendicular uniaxial alignment provided by magnetically oriented bicelles. Three (3) two-dimensional experiments have been performed using the bicelle-reconstituted Pf1 coat protein, including an ^{15}N–^{15}N correlation spectrum, a SAMPI4 spectrum (Nevzorov and Opella 2007) correlating the ^{15}N chemical shift and ^{1}H–^{15}N dipolar couplings, as well as the "spin-exchanged" version of the SAMPI4 spectrum (Nevzorov 2009). Intra-residue cross peaks have been established by cross-referencing of the three spectra. The use of sensitivity-enhanced REP-CP pulse sequence (Tang and Nevzorov 2011) further increases the signal-to-noise ratio in these experiments, and makes it possible to detect all the cross peaks for the α-helical transmembrane region (i.e. residues I22–M42). Detailed many-spin simulations have been performed to establish the optimal Hartmann-Hahn mismatch for the amide backbone ^{15}N spin correlations.

Materials and methods

A uniformly ^{15}N-labeled Pf1 phage sample was provided by Hyglos GmbH (Regensburg, Germany) at ca. 40 mg/mL total concentration of the protein. To purify Pf1 coat protein, a predefined amount of the phage was dissolved in 1 mL of TFE (50 %)/TFA (0.1 %) to precipitate the DNA, followed by lyophilization of the soluble fraction. Approximately 6 mg of the lyophilized protein was reconstituted in 180 µl solution of DMPC/DHPC (at $q = 3{:}1$ molar ratio) bicelles as previously described by Opella and co-workers (De Angelis and Opella 2007). Alternatively, an ether-linked version of DHPC, 6-*O*-PC, can be used which yields no significant differences in the observed spectra, but a much longer lifetime of the sample (Aussenac et al. 2005; De Angelis and Opella 2007). The lipid-to-protein ratio was maintained at around 55:1, and the optimal sample temperature $T = 38$ °C was found by recording the linewidths of the ^{31}P NMR lipid spectra to determine the best bicelle alignment (results not shown). All experiments have been performed on a Bruker Avance II spectrometer operating at 500 MHz ^{1}H frequency and running Topspin™ 2.0 software. A static Bruker 5 mm round-coil E-free™ probe was utilized in all experiments.

The pulse sequences used in the assignment process are shown in Fig. 1. Figure 1a depicts the homonuclear ^{15}N–^{15}N exchange experiment. Here the cross-polarization part is first applied to enhance sensitivity either by means of a single-contact CP or repetitive, REP-CP (Tang and Nevzorov 2011). Next, the ^{15}N chemical shift evolves under the conditions of proton decoupling. The proton magnetization is subsequently flipped along the *z*-direction, and an alternating 90° $-y/x$ pulse on the ^{15}N site selects either the real or imaginary component of the chemical

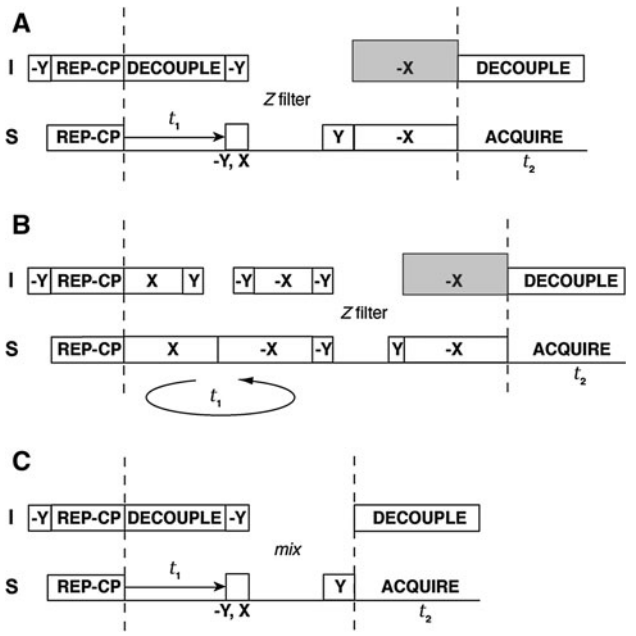

Fig. 1 Pulse sequences used for NMR spectroscopic assignment of Pf1 coat protein reconstituted in magnetically aligned DMPC/DHPC bicelles. **a** ^{15}N–^{15}N correlation pulse sequence utilizing MMHH (Nevzorov 2008; Knox et al. 2010). **b** Spin-exchanged SAMPI4 pulse sequence (Nevzorov 2009). **c** ^{15}N–^{15}N correlation pulse sequence utilizing PDSD (Marassi et al. 1999). Either conventional cross-polarization, CP, or REP-CP (Tang and Nevzorov 2011) can be used to enhance the initial ^{15}N magnetization. A 5 ms contact time was chosen for all the MMHH-based experiments, whereas a mixing time of 3 s was used for the PDSD experiment. For further details of the pulse sequences cf. the text

shift evolution. A wait time of typically less than one second is applied to eliminate any residual proton magnetization along the *x*-axis (the *Z*-filter). The proton-mediated transfer is achieved when the ^{15}N spins are brought back along the *x*-direction followed by simultaneous rf irradiation on both channels, with the rf amplitude on the ^{1}H site being higher than the Hartmann-Hahn match. Finally, the ^{15}N chemical shift is detected under the conditions of proton decoupling. Two-dimensional pulse sequence for the high-resolution separated local-field spectroscopy that simultaneously establishes internuclear correlations is depicted in Fig. 1b. As in Fig. 1a, cross-polarization is used to enhance the magnetization on the ^{15}N side. The SAMPI4 pulse sequence (Nevzorov and Opella 2007) is applied to evolve the heteronuclear dipolar couplings. After the *Z*-filter, the stored ^{15}N magnetization is brought back along the *x*-axis, and the mismatched Hartmann-Hahn scheme is applied to establish intra-residue correlations. Finally, the ^{15}N chemical shift is detected. Figure 1c shows the pulse sequence for the homonuclear exchange involving PDSD; it could also be thought as a variant of the sequence of Fig. 1a with a longer *Z*-filter, albeit without the MMHH spin exchange.

All many-spin simulations were performed using a script written in MATLAB (Mathworks, Inc.). The data have been processed using NMRPipe (Delaglio et al. 1995).

Results and discussion

Simulations of spin dynamics for the perpendicular bicelles

A theoretical framework for the magnetization exchange between two dilute spins surrounded by a proton bath under mismatched Hartmann-Hahn conditions has been previously described (Nevzorov 2008, 2009; Traaseth et al. 2010). Such a framework allows for theoretical simulations of the mismatch conditions, thus considerably shortening experimental optimizations. Using the crystal structures of NAL (Nevzorov 2009; Traaseth et al. 2010) and NAVL (Traaseth et al. 2010) simulations have been shown to accurately describe the experimental behavior such as the cross-peak intensity as a function of the B_1 field mismatch between the proton and ^{15}N rf fields, ^{15}N spin-lock rf field strengths, and the total irradiation time. Experiments performed on single crystals and the simulations demonstrate the capability of establishing cross peaks between the dilute spins separated by as far as 6.7 Å (Nevzorov 2008), which may give rise to long-distance (e.g. i, $i + 2$) correlations in the spin-dense protein backbones and multiple cross peaks, thus potentially making the use of MMHH method difficult for sequence-specific assignment. Contrary to this expectation, however, it was shown experimentally (Knox et al. 2010), that the cross-peak resonances for a uniformly labeled sample generally follow the (i, $i + 1$) pattern, thus making the MMHH scheme suitable for spectroscopic assignment. Here we have performed detailed many-spin simulations in order to optimize the experiment for the case of Pf1 coat protein reconstituted in bicelles, and to explore the potential evolution of the long-range cross peaks using the spectroscopic assignment and structural coordinates from previous studies (Thiriot et al. 2005; Opella et al. 2008; Park et al. 2010). Briefly, the spin system evolves under the Hamiltonian (Nevzorov 2008):

$$H = \omega_S S_x^{total} + \omega_I I_x^{total} + \sum_{k=1}^{N_S}\sum_{n=1}^{N_I} a_{kn} S_z^{(k)} I_z^{(n)} + \sum_{i<j}^{N_I} b_{ij}\left[I_z^{(i)} I_z^{(j)} - \frac{1}{4}\left(I_+^{(i)} I_-^{(j)} + I_-^{(i)} I_+^{(j)}\right)\right] \quad (1)$$

And the magnetization transferred to the k'th nitrogen spin is obtained by using a trace metric expression:

$$\left\langle S_x^{(k)} \right\rangle = Trace\left(S_x^{(k)} e^{-iHt} \rho(0) e^{iHt}\right) \quad (2)$$

where the initial density matrix corresponds to the "normalized" magnetization at the starting spin (denoted as the first nitrogen), and is given by:

$$\rho(0) = S_x^{(1)} / 2^{N-2} \quad (3)$$

Two or three ($N_S = 2$, 3) nitrogen, or S, spins were considered in the simulations; N_I is the total number of protons, I. The radiofrequency (rf) irradiation amplitudes of the low (S) and high spins (I) are given by ω_S and ω_I, respectively. The interaction constants between the S-spins and N_I protons are given by a_{kn}, and b_{ij} describe the interactions among the protons. To calculate the interaction constants, the atomic coordinates were taken from the three-dimensional structure of Pf1 coat protein (PDB ID 1ZN5) (Thiriot et al. 2005). Only the transmembrane residues were considered (from I22 to M42 in the present simulations), and the effect of the perpendicular orientation and uniaxial rotation in bicelles was treated by scaling the dipolar couplings by −0.4 (Park et al. 2006b). The amide protons and the alpha-protons were always included, and the other protons were retained if their dipolar couplings to the nitrogen spins of interest were greater than a certain cutoff value (generally around 100 Hz, depending on a residue) to yield the desired number of protons for the simulation ($N_I = 10$ in the present study, thus making it a system of up to $N = 13$ spins total). The magnetization transfer amplitudes were calculated at various values of ω_S and ω_I for the mixing time 10 ms (sufficient to achieve a quasi-stationary equilibrium for the transfer). The magnetization amplitudes were normalized relative to the main peak intensity in the absence of the exchange, cf. Eq. 3. The transfers were calculated starting at each amide nitrogen in the sequence of Pf1 corresponding to the transmembrane region, (i.e. from I22 to M42) and the transfer profiles were then averaged across the entire structure. The ^{1}H spin lock values were varied from −10 to +10 kHz relative to the ^{15}N spin lock. Figure 2a shows the simulations for the values of $\omega_S/2\pi$ equal to 20, 40, and 60 kHz. Here, only isolated pairs of the nitrogen spins were considered at a time ($N_S = 2$). The transfers calculated for the (i, $i + 1$) and (i, $i + 2$) magnetization pathways are shown in Fig. 2a for the various values of ω_S. The isolated-pair simulations predict that the average (i, $i + 2$) transfer intensity is about half of that for the (i, $i + 1$) cross peak (at its maximum value), which would imply that the experimental conditions can be adjusted accordingly by varying the mismatch rf amplitudes to minimize the evolution of long-range interactions. Moreover, a slight increase in the optimal transfer efficiency with decreasing

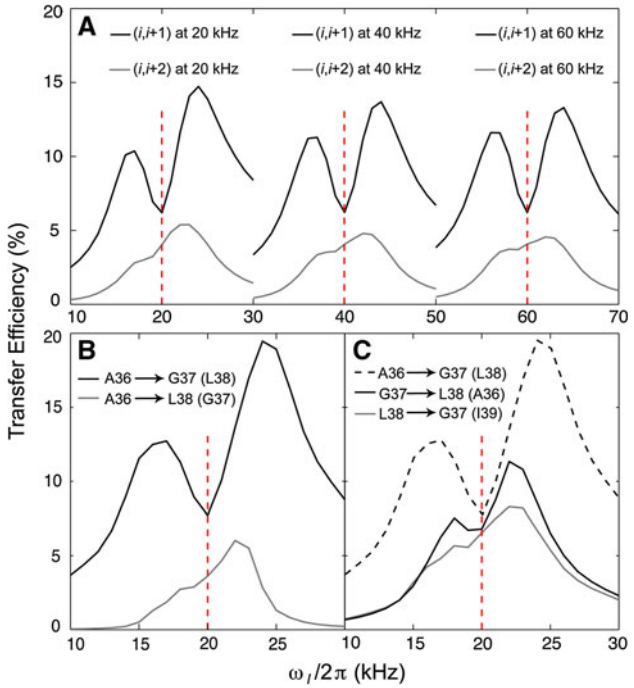

Fig. 2 Simulations of the efficiency of magnetization transfer between the rare ^{15}N spins under the MMHH conditions. **a** $N = 12$ spin simulations including single pairs of amide ^{15}N spins for Pf1 reconstituted in bicelles (with the coordinates for residues I22–M42 taken from PDB ID 1ZN5, cf. the text) comparing the $(i, i + 1)$ and $(i, i + 2)$ magnetization exchange pathways at 20, 40, and 60 kHz ^{15}N spin-lock B_1 fields (marked by *vertical dotted lines*). Values were averaged across the transmembrane region (residues 22–42). At 20 kHz ^{15}N spin lock B_1 field, the optimal transfer is enhanced by ca. 5.5 and 7.5 % over the 40 and 60 kHz ^{15}N spin lock rf fields respectively (cf. Traaseth et al. 2010). **b** Three-^{15}N spin ($N = 13$) simulations examining the effects of spin competition on the long-range $(i, i + 2)$ magnetization transfer in the presence of the more preferential $(i, i + 1)$ pathway. The $(i, i + 2)$ magnetization transfer between two representative residues A36 and L38 (in the presence of a competing nitrogen spin at G37; *gray line*) is compared to the A36–G37 $(i, i + 1)$ transfer (*black line*). The efficiency of the $(i, i + 2)$ transfer in the presence of the competing $(i, i + 1)$ pathway is even lower than in part (**a**). **c** Three-^{15}N spin ($N = 13$ total number of spins) simulations comparing the magnetization build up and demonstrating the effect of competing spins on the $(i, i + 1)$ and $(i + 1, i)$ cross-peak intensities as a function of the rf amplitude mismatch. The transfer from the nitrogen spin at G37 to that of L38 (in the presence of A36; *black line*) and the transfer from L38 to G37 (in the presence of I39; *gray line*) have been considered. The A36–G37 transfer from part B is also shown here (*black dashed line*) to compare it to the L38–G37 transfer

^{15}N spin-lock B_1 rf field has been observed as in the previous crystal studies (Traaseth et al. 2010).

Furthermore, an important theoretical observation is unequal intensities of the cross peaks, which can be explained by spin competition owing to the non-commuting character of the dipolar interaction terms involved in the Hamiltonian, Eq. 1. For instance, the amide nitrogen spin of residue L38 competes with that of A36 for the polarization originating at G37, while G37 competes with I39 for the polarization from L38, which can result in different cross peak intensities for the bi-directional exchange between the corresponding pairs of residues. The spin competition can be further used to explain the low probability of occurrence of long-range (e.g. i, $i \pm 2$) correlations, considering that the $(i, i \pm 2)$ spin system would have to compete with the more preferential $(i, i + 1)$ and $(i, i - 1)$ transfer pathways. A series of simulations were run to explore the above effects of spin competition along the backbone of Pf1. However, within the computer memory limitations, only a single competing spin could be considered in addition to the main transfer pathway (yielding a $N = 13$ spin system total). Figure 2b shows the intensity profiles calculated for the $(i, i + 2)$ transfers from residue A36 to L38 (gray line) in the presence of the competing $(i, i + 1)$ pathway for the transfer from A36 to G37 (shown by the black line). It can be seen that the more predominant $(i, i + 1)$ pathway substantially lowers the efficiency of the long distance $(i, i + 2)$ transfer, thus making the differences between the $(i, i + 1)$ and $(i, i + 2)$ cross peaks even more pronounced than in Fig. 2a. This theoretical result shows that, for a uniformly ^{15}N labeled protein, most if not all of the crosspeaks are expected to be for an $(i, i \pm 1)$ transfer, thus making the MMHH scheme suitable for the sequential assignment of ^{15}N amide backbone resonances. Moreover, unequal intensities can be expected even for the $(i, i \pm 1)$ cross peaks, which may be due to different spin-density distributions of the side-chain protons participating in the MMHH transfer. To illustrate this effect, the profiles shown in Fig. 2c contain a representative $(i, i + 1)$ magnetization transfer from residue G37 to L38 in the presence of the competing $(i, i - 1)$ transfer to the amide nitrogen of A36 (black line), and from residue L38 to G37 in the presence of the amide nitrogen from residue I39 (gray line). As can be seen, the presence of a competing pathway may result in slightly unequal intensities of the cross peaks that are symmetrically positioned with respect to the main diagonal in a homonuclear spin-exchange spectrum. In addition, shown in Fig. 2c by the black dashed line is the same A36-G37 transfer as in Fig. 2b, but now it is to be compared to the L38–G37 transfer. It can be seen that even at the optimal MMHH conditions, the latter has a much lower intensity (about 12 %) as compared to the A36–G37 transfer (about 20 %). This unequal intensity of the cross peaks is fully supported by the experimental observations (see below). Such an intensity contrast can be used in disambiguation of the cross peaks during the assignment process.

Experimental results

Figure 3a shows the ^{15}N–^{15}N correlation spectrum of uniformly ^{15}N–labeled Pf1 coat protein reconstituted in

magnetically aligned DMPC/DHPC bicelles acquired using the pulse sequence of Fig. 1a (cf. figure captions for detailed listings of the experimental parameters). Figure 3b (red contours) shows the SAMPI4 (Nevzorov and Opella 2007) spectrum. The SAMPI4 spectrum is overlaid with its spin-exchanged version (blue contours) acquired using the pulse sequence shown in Fig. 1b. The t_1 dimension of the latter is evolved using SAMPI4, followed by the *Z*-filter and the proton-mediated MMHH spin exchange, during which the proton rf amplitude is set above the Hartmann-Hahn matching condition (Knox et al. 2010). The choice for the optimal mismatch conditions is provided by the simulations as demonstrated in the previous section (cf. Fig. 2a). From the simulations, the optimal mismatch amplitude to evolve the $(i, i + 1)$ correlations was found to be at 5–6 kHz above the exact Hartmann-Hahn match. Overlaying the spectra with and without spin exchange in Fig. 3b allows for the cross-peaks to be distinguished from the main peaks, and the sequential connectivity among the latter to be established. Note that the exchanged SAMPI4 spectrum exhibits somewhat broader linewidths in the dipolar (indirect) dimension than the SAMPI4, which may be due to the more prolonged sample heating during the MMHH exchange (5 ms). This, in turn, may change the B_1 rf fields at the sample, thus making the homonuclear decoupling during the dipolar evolution somewhat less efficient. In addition, some broader peaks may be due to the overlapping cross- and main-peaks.

As can be seen from Fig. 3 (where the red boxes are used to depict the i, $i + 1$ connectivities) many of the spectral assignments can be established by associating the cross peaks with the corresponding main peaks. For clarity, the results for the sequential residues V35–A36, A36–G37, G37–L38, L38–I39, I39–Y40, Y40–S41 and S41–M42 are highlighted. Figure 3c, d show digitized versions of the experimental spectra of Fig. 3a, b to facilitate the visualization of the assignment process. It is important to note that the combination of the homonuclear ^{15}N–^{15}N spin-exchange spectrum (Fig. 3a, c) and the spin-exchange SAMPI4 spectrum (Fig. 3b, d) assists in resolving ambiguities when the main peaks in the latter spectrum have similar dipolar couplings. Furthermore, unequal relative intensities of the cross peaks can further aid in their disambiguation (see simulations in Fig. 2c). For example, there are several assignment possibilities for the cross peak of G37, since there are three (3) main peaks that have the same dipolar couplings in the SAMPI4 spectrum (at around 2.1 kHz). However, upon the cross-referencing of the corresponding chemical shifts and the stronger cross peak in the ^{15}N–^{15}N exchange spectrum, only one possibility remains, which leads to the assignment: A36–G37 (at 94.8 and 64.6 ppm, respectively). All the other possibilities are ruled out. Note that the simulations of Fig. 2c also predict that the intensity of the cross peak corresponding to the A36–G37 transfer is greater than that for the L38–G37 transfer, which may point at a role of the side-chain protons in the $(i, i + 1)$ MMHH transfer. This strategy, however, requires absolute assignment of at least one "seed" residue; in the present illustrative case we have used the previously established assignment for G37 (Opella et al. 2008; Park et al. 2010). Alternatively, a single selectively labeled spectrum including all Alanines, Glycines, and Leucines could be used to immediately assign the residues A36–G37–L38 (there is only one such combination in the primary sequence for the Pf1 coat protein). This would serve as a starting point for the assignment; such a choice for the selective labeling is clearly sequence-dependent. Notably, these assignments are in agreement with those obtained previously using a combination of selective isotopic labeling and the shotgun approach (Opella et al. 2008; Park et al. 2010), and the cross-peaks generally follow the $(i, i + 1)$ connectivity pattern. Similar process can also be applied to the remaining residues in the transmembrane domain, including Y25–G28 and others (cf. Fig. 3c). However, since the peaks for G28 and A29 have nearly identical ^{15}N chemical shifts, detection of the cross peaks between these two residues using the two-dimensional spectra is not feasible, which breaks down the continuity of the assignment process. Therefore, complete assignment of NMR spectra of oriented membrane proteins would likely require performing three-dimensional double-resonance experiments, as done routinely in MAS and liquids NMR.

To further improve the quality of the spectra, the newly established REP-CP sequence (Tang and Nevzorov 2011) can be employed to significantly (up to 40 %) increase the signal-to-noise ratio for the highly dynamic membrane proteins reconstituted in perpendicular bicelles. Moreover, with the enhanced signal-to-noise ratio, much longer (up to 20 ms) acquisition intervals in the direct dimension can be used to help eliminate the spectral crowdedness near the diagonal region in the homonuclear spin-exchanged spectra. As can be seen from Fig. 4a, the resonance lines in the ^{15}N–^{15}N correlation spectrum are much narrower than those obtained in the previous spectra (cf. Fig. 3a), hence making the cross-peak detection more reliable. A side-by-side comparison was performed between two spin-exchange experiments involving either MMHH (Fig. 4a) or PDSD (Fig. 4b) during the mixing period (with the pulse sequence for the latter shown in Fig. 1c). For the MMHH spin-exchange experiment, 512 transients were co-added, 5 ms contact time with a Z filter of 0.5 s were used (yielding the total time 6 days 18 h). For the PDSD spin-exchange experiment, 256 scans and a mixing time of 3 s were utilized (yielding the total time 4 days 13 h). In both experiments, 80 complex t_1 points, five repetitive contacts, and a 6 s recycle delay were employed. During the MMHH

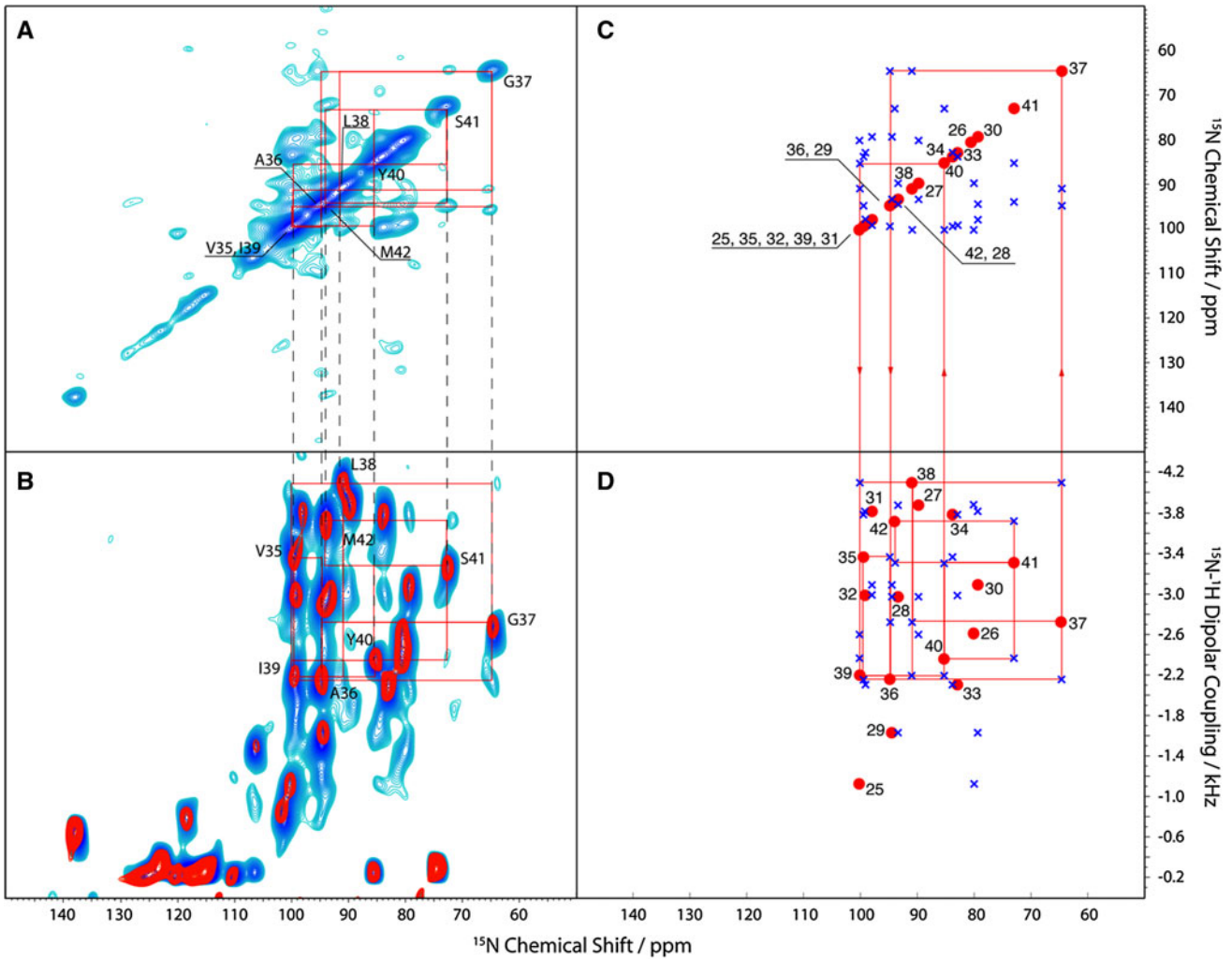

Fig. 3 Spectra of Pf1 coat protein reconstituted in magnetically aligned DMPC/DHPC bicelles at $T = 38$ °C. **a** Experimental ^{15}N–^{15}N spin correlation spectrum: 512 scans; MMHH at 45.5 kHz ^{15}N B_1 rf field and 51.5 kHz ^{1}H B_1 field, 0.5 s *Z*-filter and 5 ms mixing time; 64 complex t_1 points; **b** Experimental SAMPI4 spectrum (*red*) overlaid with its spin-exchange version (*blue*). SAMPI4: 128 scans, 45.5 kHz B_1 field (for CP match and decoupling), 80 real t_1 points (*red contours*); Spin-exchanged SAMPI4: 1024 scans, MMHH at 45.5 kHz ^{15}N B_1 rf field and 51.5 kHz ^{1}H B_1 field, 0.5 s *Z*-filter and 5 ms mixing time; 80 real t_1 points (*blue contours*). A single-contact CP of 1 ms, 10 ms total acquisition time in the indirect dimension, and a 6 s recycle delay were used in all experimental spectra. *Darker shadows* of *blue* in the spectra indicate higher intensity of the resonance lines, whereas *lighter shadows* correspond to less intense areas. **c** Digitized version of the ^{15}N–^{15}N spin correlation spectrum. **d** Digitized version of the SAMPI4 spectra. Cross-referencing among the three experimental spectra allows one to obtain connectivities between the consecutive residues as shown by the *red boxes*. For clarity, a representative assignment pathway for residues V35–M42 is shown in the digital versions of the spectra (parts **c** and **d**). The cross-peaks for other residues can also be established

exchange, the absolute Hartmann-Hahn match amplitudes were lowered to the value of about 20 kHz, following the previous studies (Traaseth et al. 2010; Khitrin et al. 2011), while the B_1 amplitude mismatch for the protons was still kept at 5 kHz. An additional benefit of lowering the B_1 amplitudes is a reduced sample heating during the MMHH exchange and the subsequent 20 ms acquisition under the conditions of proton decoupling. A comparison of Fig. 4a, b shows that the MMHH method yields a better resolution for both the main and cross peaks, especially near the main diagonal. The signal-to-noise ratio for the well-resolved representative cross peaks was estimated to be between 3:1 and 5:1 in both spectra. However, upon closer examination of the PDSD spectrum, it becomes evident that some of the cross peaks, such as that corresponding to G37–L38, are not evolved at all when using the PDSD method. In addition, the main peaks corresponding to the more dynamic N-terminal region are entirely missing in the PDSD spectrum, cf. Fig. 4a, b.

Shown in Fig. 5 is a symmetrized ^{15}N–^{15}N correlation experiment of Fig. 4a. Red crosses show the simulated cross peaks whose chemical shifts are taken from the

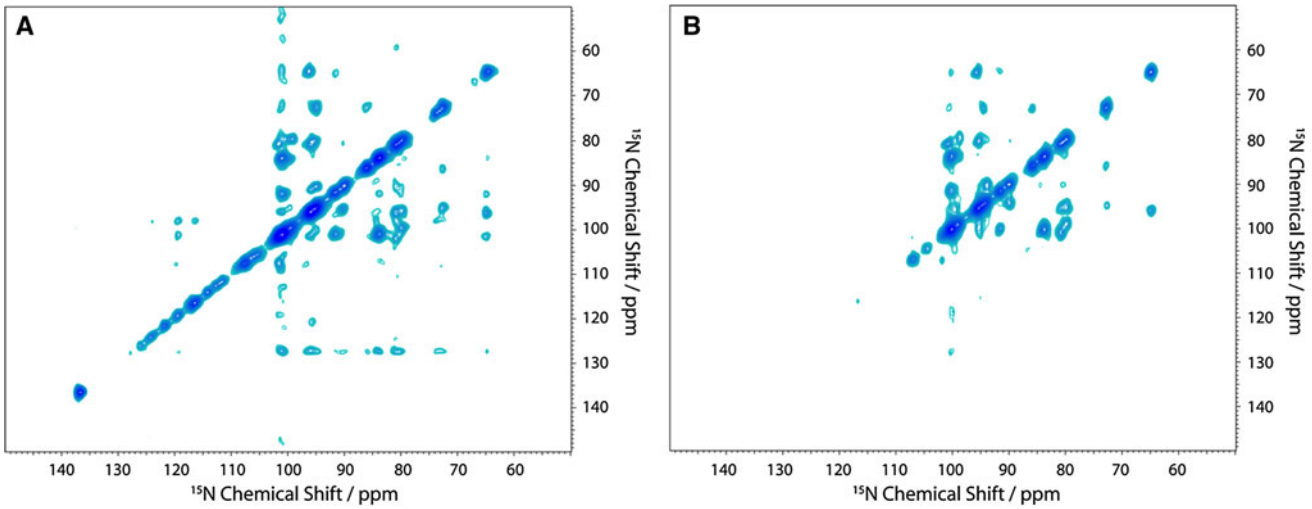

Fig. 4 A comparison between **a** ^{15}N–^{15}N MMHH spin-exchange spectrum at 512 scans, 20 kHz ^{15}N B_1 rf field and 25 kHz ^{1}H B_1 field, and 0.5 s *Z*-filter; and **b** ^{15}N–^{15}N PDSD spectrum: 256 scans and 3 s mixing time. The REP-CP pulse sequence with 5 contacts of 300 μs length each was used to enhance magnetization on the ^{15}N spins (Tang and Nevzorov 2011), 80 complex t_1 points, 20 ms total acquisition time in the direct dimension, and a 6 s recycle delay were used in both spectra. In part **b**, the peaks are slightly broader, and some of them (both the main and cross-peaks) are missing in the spectrum

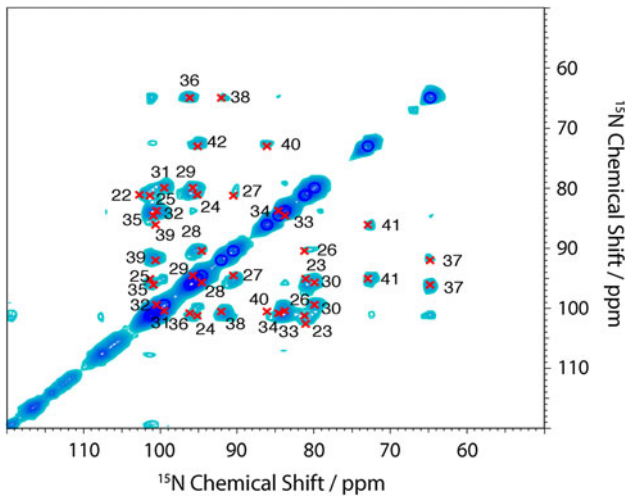

Fig. 5 A zoomed-in view of the symmetrized ^{15}N–^{15}N MMHH exchange spectrum from Fig. 4a overlaid with the simulated cross-peaks (*red crosses*) calculated using the chemical shifts from the main peaks of the SAMPI4 spectrum (from Fig. 3d) and the previous assignment (Opella et al. 2008; Park et al. 2010). All simulated cross-peaks have underlying intensity, which proves the correctness of the previous assignment. Moreover, the cross-peaks generally follow the (i, $i + 1$) connectivity pattern

corresponding SAMPI4 spectrum (the main peaks of Fig. 3d) using the previous assignment (Opella et al. 2008; Park et al. 2010; Lu et al. 2011). As can be seen from Fig. 5, all simulated cross peaks have an underlying experimental intensity, which in turn, proves the correctness of the previous assignment (Opella et al. 2008; Park et al. 2010; Lu et al. 2011). However, there are also additional weaker cross peaks that may correspond to the long-distance (i.e. i, $i + 2$) correlations; the cross peak between G37 and I39 is one such example. We note that these extra peaks may not evolve when using higher B_1 rf fields and mismatches (cf. the simulations in Fig. 2a and the experimental spectrum of Fig. 3a); this issue merits further investigation.

Conclusions

Oriented-sample solid-state NMR represents a powerful technique for the structural studies of the conformations of membrane proteins in their native-like, fully hydrated lipid environment. In the present work, a purely spectroscopic method for establishment and validation of the NMR assignments for membrane proteins reconstituted in magnetically aligned bicelles has been presented. The quality of the spin-correlation spectra previously obtained for Pf1 reconstituted in magnetically aligned bicelles (Knox et al. 2010) have been significantly improved. Furthermore, we have provided an assignment strategy for the uniformly ^{15}N labeled Pf1 phage coat protein reconstituted in "perpendicular" bicelles by using three two-dimensional experiments that could greatly reduce the number of selectively labeled samples utilized in the assignment process. We have demonstrated the general applicability of the proton-mediated magnetization transfer under the MMHH conditions (Nevzorov 2008; Knox et al. 2010) for establishing predominantly the (i, $i + 1$) spin correlations. Many-spin simulations accurately predict the optimal mismatch B_1 field amplitudes without the necessity of running lengthy experimental optimizations. The sample of Pf1 coat protein reconstituted in perpendicular bicelles

provides sufficient resolution to resolve nearly all of the sequential cross peaks in the transmembrane region. Moreover, sensitivity enhancement afforded by the REP-CP sequence allows one to perform longer (up to 20 ms) acquisitions in the homonuclear ^{15}N–^{15}N exchange experiments. Since the MMHH exchange is driven by the dipolar couplings, its use is primarily restricted to the more rigid regions of the protein. Furthermore, the ability of the MMHH scheme to establish correlations among the dilute spins separated by as far as 6.7 Å (Nevzorov 2008, 2009; Traaseth et al. 2010), may make it possible to elucidate the intermolecular contacts between the transmembrane alpha-helices, which calls for further investigation. The method has confirmed the previous assignment for the transmembrane region (Opella et al. 2008; Lu et al. 2011) that was performed using multiple selectively labeled samples. Notably, the present assignment method allows one to use a uniformly ^{15}N labeled sample, with perhaps only a few selectively labeled "seed" spectra to initiate the assignment process. However, for structure determination and complete NMR assignment for membrane proteins of more complex topology, doubly labeled samples and three-dimensional pulse sequences incorporating the MMHH spin exchange may be necessary. Recent studies (Lin and Opella 2011) correlating the ^{13}C and ^{15}N spins via the MMHH mechanism are especially encouraging in this regard.

Acknowledgments We would like to thank Prof. Stanley J. Opella and George J. Lu (UCSD) for stimulating discussions. Research supported by a grant from NSF (MCB 0843520).

References

Aussenac F, Lavigne B, Dufourc EJ (2005) Toward bicelle stability with ether-linked phospholipids: temperature, composition, and hydration diagrams by H-2 and P-31 solid-state NMR. Langmuir 21(16):7129–7135

Cady SD, Hong M (2009) Effects of amantadine on the dynamics of membrane-bound influenza A M2 transmembrane peptide studied by NMR relaxation. J Biomol NMR 45(1–2):185–196

De Angelis AA, Opella SJ (2007) Bicelle samples for solid-state NMR of membrane proteins. Nat Protoc 2(10):2332–2338

De Angelis AA, Howell SC, Opella SJ (2006) Assigning solid-state NMR spectra of aligned proteins using isotropic chemical shifts. J Magn Reson 183(2):329–332

Delaglio F, Grzesiek S, Vuister GW, Zhu G, Pfeifer J, Bax A (1995) NMRPipe: a multidimensional spectral processing system based on Unix pipes. J Biomol NMR 6(3):277–293

Glover KJ, Whiles JA, Wu GH, Yu NJ, Deems R, Struppe JO, Stark RE, Komives EA, Vold RR (2001) Structural evaluation of phospholipid bicelles for solution-state studies of membrane-associated biomolecules. Biophys J 81(4):2163–2171

Khitrin AK, Xu JD, Ramamoorthy A (2011) Cross-correlations between low-gamma nuclei in solids via a common dipolar bath. J Magn Reson 212(1):95–101

Knox RW, Lu GJ, Opella SJ, Nevzorov AA (2010) A resonance assignment method for oriented-sample solid-state NMR of proteins. J Am Chem Soc 132(24):8255–8257

Lewandowski JR, De Paepe G, Griffin RG (2007) Proton assisted insensitive nuclei cross polarization. J Am Chem Soc 129(4):728–729

Lin EC, Opella SJ (2011) (1)H assisted (13)C/(15)N heteronuclear correlation spectroscopy in oriented sample solid-state NMR of single crystal and magnetically aligned samples. J Magn Reson 211(1):37–44

Lu GJ, Son WS, Opella SJ (2011) A general assignment method for oriented sample (OS) solid-state NMR of proteins based on the correlation of resonances through heteronuclear dipolar couplings in samples aligned parallel and perpendicular to the magnetic field. J Magn Reson 209(2):195–206

Marassi FM (2001) A simple approach to membrane protein secondary structure and topology based on NMR spectroscopy. Biophys J 80(2):994–1003

Marassi FM, Opella SJ (2000) A solid-state NMR index of helical membrane protein structure and topology. J Magn Reson 144(1):150–155

Marassi FM, Gesell JJ, Valente AP, Kim Y, Oblatt-Montal M, Montal M, Opella SJ (1999) Dilute spin-exchange assignment of solid-state NMR spectra of oriented proteins: acetylcholine M2 in bilayers. J Biomol NMR 14(2):141–148

Mote KR, Gopinath T, Traaseth NJ, Kitchen J, Gor'kov PL, Brey WW, Veglia G (2011) Multidimensional oriented solid-state NMR experiments enable the sequential assignment of uniformly (15)N labeled integral membrane proteins in magnetically aligned lipid bilayers. J Biomol NMR 51(3):339–346

Nambudripad R, Stark W, Opella SJ, Makowski L (1991) Membrane-mediated assembly of filamentous bacteriophage Pf1 coat protein. Science 252(5010):1305–1308

Nevzorov AA (2008) Mismatched Hartmann-Hahn conditions cause proton-mediated intermolecular magnetization transfer between dilute low-spin nuclei in NMR of static solids. J Am Chem Soc 130(34):11282–11283

Nevzorov AA (2009) High-resolution local field spectroscopy with internuclear correlations. J Magn Reson 201(1):111–114

Nevzorov AA (2011) Orientational and motional narrowing of solid-state NMR lineshapes of uniaxially aligned membrane proteins. J Phys Chem B 115(51):15406–15414

Nevzorov AA, Opella SJ (2007) Selective averaging for high-resolution solid-state NMR spectroscopy of aligned samples. J Magn Reson 185(1):59–70

Opella SJ, Zeri AC, Park SH (2008) Structure, dynamics, and assembly of filamentous bacteriophages by nuclear magnetic resonance spectroscopy. Annu Rev Phys Chem 59:635–657

Park SH, Mrse AA, Nevzorov AA, De Angelis AA, Opella SJ (2006a) Rotational diffusion of membrane proteins in aligned phospholipid bilayers by solid-state NMR spectroscopy. J Magn Reson 178(1):162–165

Park SH, De Angelis AA, Nevzorov AA, Wu CH, Opella SJ (2006b) Three-dimensional structure of the transmembrane domain of Vpu from HIV-1 in aligned phospholipid bicelles. Biophys J 91(8):3032–3042

Park SH, Marassi FM, Black D, Opella SJ (2010) Structure and dynamics of the membrane-bound form of Pf1 coat protein: implications of structural rearrangement for virus assembly. Biophys J 99(5):1465–1474

Prosser RS, Hunt SA, DiNatale JA, Vold RR (1996) Magnetically aligned membrane model systems with positive order parameter: switching the sign of S-zz with paramagnetic ions. J Am Chem Soc 118(1):269–270

Sanders CR, Hare BJ, Howard KP, Prestegard JH (1994) Magnetically-oriented phospholipid micelles as a tool for the study of membrane-associated molecules. Prog Nucl Magn Reson Spectrosc 26:421–444

Suter D, Ernst RR (1985) Spin diffusion in resolved solid-state NMR-spectra. Phys Rev B 32(9):5608–5627

Tang WX, Nevzorov AA (2011) Repetitive cross-polarization contacts via equilibration-re-equilibration of the proton bath: sensitivity enhancement for NMR of membrane proteins reconstituted in magnetically aligned bicelles. J Magn Reson 212(1):245–248

Thiriot DS, Nevzorov AA, Opella SJ (2005) Structural basis of the temperature transition of Pf1 bacteriophage. Protein Sci 14(4): 1064–1070

Traaseth NJ, Gopinath T, Veglia G (2010) On the performance of spin diffusion NMR techniques in oriented solids: prospects for resonance assignments and distance measurements from separated local field experiments. J Phys Chem B 114(43):13872–13880

Wang J, Denny J, Tian C, Kim S, Mo Y, Kovacs F, Song Z, Nishimura K, Gan Z, Fu R, Quine JR, Cross TA (2000) Imaging membrane protein helical wheels. J Magn Reson 144(1):162–167

Xu JD, Smith PES, Soong R, Ramamoorthy A (2011) A proton spin diffusion based solid-state NMR approach for structural studies on aligned samples. J Phys Chem B 115(16):4863–4871